

## Nonadiabatic superconductivity: The role of van Hove singularities

E. Cappelluti and L. Pietronero

*Dipartimento di Fisica, Università di Roma "La Sapienza," Piazzale Aldo Moro 2, I-00185 Roma, Italy  
and Istituto Nazionale di Fisica della Materia, Sezione di Roma, Roma, Italy*

(Received 6 July 1995)

We consider the effect of van Hove singularities in the density of states (DOS) on the generalized theory of superconductivity that includes the first contribution beyond Migdal's theorem (nonadiabatic). Most of our results are not specific to a van Hove singularity and can be extended to the generic situation in which the Fermi surface is close to a peak in the DOS. Often the effect of a peak in the DOS is discussed in terms of an enhancement of the electron-phonon coupling  $\lambda$  using the standard theory. Here we point out that in the most interesting situations this peak structure unavoidably leads to a breakdown of Migdal's theorem because the effective range of electronic energies becomes very narrow. We include therefore the first diagrams beyond Migdal's theorem that lead to a change in the structure of the theory and not just on the value of the effective coupling. These nonadiabatic effects lead naturally to an enhancement of the value of  $T_c$  with respect to the adiabatic theory with the same coupling. This enhancement is mainly due to the predominant role of small momentum scattering that is a consequence of the peak in the DOS. These results provide therefore a perspective for the effects of DOS peaks in the theory of superconductivity.

### I. INTRODUCTION

The idea that density of state (DOS) peaks may be important for superconductivity (SC) was first considered for A15 compounds that showed one-dimensional features.<sup>1</sup> In the context of high- $T_c$  superconductivity, the planar structure of the CuO<sub>2</sub> layers leads naturally to a van Hove (logarithmic) singularity of the DOS that could be coincident or very close to the Fermi energy, depending on the doping. This situation has led various authors to reconsider in greatest detail the possible effects of DOS peaks in superconductivity, both for phonon mediators as well as for other mechanism.<sup>2</sup>

The basic concept is that a peak in the DOS may correspond to a large value of the effective electron-phonon coupling  $\lambda = 2g^2N(0)/\omega_0$ , when  $N(0)$  is the effective DOS at the Fermi level.<sup>3,4</sup> Of course, this leads to various ambiguities because the previous expression of  $\lambda$  corresponds to a flat DOS. In case of sharp peaks, the value of  $N(0)$  may even diverge, but this should then be replaced by an effective  $N(0)$  that corresponds to some averaged DOS over an energy window defined by the phonon frequency.<sup>3</sup> In this perspective, therefore, the effect of the structure in the DOS is simply to produce a large value of  $\lambda$ . A peak in the DOS, however, leads inevitably to complications with respect to the structure of the theory. For example, if the peak structure is correctly considered within a BCS framework, one obtains a different expression for the transition temperature that does not correspond just to a change of  $\lambda$ . This point of view was developed first by Hirsch and Scalapino<sup>5</sup> in the context of a BCS approach for an attractive Hubbard interaction, and it was later discussed also for the phonon coupling.<sup>6-8</sup> In this case one obtains

$$T_c \sim T_F \exp \left[ - \sqrt{\frac{2}{\lambda} + \ln^2 \left( \frac{K_B T_F}{\hbar \omega_D} \right)} \right], \quad (1.1)$$

where  $T_F$  is the Fermi temperature and  $\omega_D$  the Debye frequency. In the nonadiabatic limit ( $\omega_D \approx T_F$ ), one recovers the

result of Ref. 5. The expression given by Eq. (1.1) shows interesting modification not only for the effective coupling, but also for the isotopic effect that is now substantially reduced. On the other hand, in the adiabatic limit ( $\omega_D \ll T_F$ ) one recovers the standard BCS expression with an effective coupling,

$$\lambda_E = \lambda \ln \left( \frac{K_B T_F}{\hbar \omega_D} \right), \quad (1.2)$$

where  $\lambda$  is the coupling that would be obtained in the case of a constant DOS with the same total number of states.

A next step has been the introduction of retardation effects by considering a ladder equation for the gap with the use of Green's functions.<sup>9</sup> The results are mainly numerical and, for weak coupling, essentially confirm the behavior of Eq. (1.1), but identify also the strong-coupling behavior. The presence of a peak in the DOS, however, unavoidably leads into complications with respect to the adiabatic hypothesis and Migdal's theorem.<sup>10</sup> In fact, the possible enhancement of  $T_c$  is due to the nonadiabatic limit [Eq. (1.1)] or, analogously, to a strong-coupling (divergent) limit in the adiabatic regime [Eq. (1.2)]. In both situations it is important to consider effects that are beyond Migdal's theorem, like vertex and cross corrections. A simple estimate of these effects has been performed in Ref. 12. The conclusion of this work was that vertex and cross corrections decrease the enhancement of the transition temperature corresponding to the van Hove singularity in the DOS.

The problem of the breakdown of Migdal's theorem has been recently receiving more and more attention in relation to both phonon and nonphonon mediators.<sup>13</sup> In the past few years, we have considered the generalization of the many-body theory of superconductivity beyond Migdal's theorem in a rather systematic way. These studies were mainly motivated by the fact that in all high- $T_c$  superconductors, from the oxides to the C<sub>60</sub> compounds, phonon frequencies are of the order of Fermi energy.<sup>13</sup> This leads to a generalization of

Eliashberg equations<sup>11</sup> to include vertex corrections and other nonadiabatic effects.<sup>14–17</sup> We have shown that these effects have a complex structure in *frequency* and *momentum* of the exchanged phonon. This point was not appreciated before because the momentum dependence was usually neglected as in Ref. 12. This complex structure can lead to positive and negative effects with respect to  $T_c$ . In particular, if small momentum scattering is predominant, the value of  $T_c$  can be appreciably enhanced. This situation can be realized if one considers the effects of Coulomb correlations in the el-ph scattering process. An alternative possibility, however, could be to have peak structures in the DOS. Recently, it has been also pointed out that peaks or singularities in the DOS near the Fermi energy can induce a modulation of the momentum dependence for the electron-phonon coupling.<sup>18</sup> This is a very important point because we are going to see that, if Migdal's theorem does not hold, peaks in the DOS associated with a modulation of the el-ph coupling can play a very important role by enhancing  $T_c$ .

The purpose of this paper therefore is to analyze, at the same level of completeness of Refs. 16, 17, the problems posed by peaks in the DOS beyond Migdal's theorem. In particular, we shall focus mainly on the van Hove singularity, but our results could be easily extended to other types of peaks structures.

## II. IDENTIFICATION OF THE EFFECTIVE ELECTRON-PHONON COUPLING FOR SYSTEMS WITH A VAN HOVE SINGULARITY

In discussing the effect of peak structures in the density of states, it is important to introduce the correct definition for the effective electron-phonon coupling. This is essential in order to be able to make meaningful comparisons between different approaches and results. The point is that the usual simple standard definition  $\lambda = 2g^2N(0)/\omega_0$  is based on the assumption of a structureless DOS. The question of its generalization in the case of strong fluctuations in the DOS is not trivial and requires a careful analysis.

Within the Eliashberg approach, the correct  $\lambda$  is the one that can be related to the experimental Eliashberg function  $\alpha^2F(\omega)$  via the expression

$$\lambda = \int_0^\infty \frac{2\alpha^2F(\omega)}{\omega} d\omega, \quad (2.1)$$

in which we use the standard notations.<sup>19</sup> For a flat band, Eq. (2.1) corresponds also to  $\lambda = 2g^2N(0)/\omega_0$ . The generalization, however, has to start from Eq. (2.1), which defines  $\lambda$  in an unambiguous way, independently of the eventual structure of the DOS.

It can be shown that Eq. (2.1) is also equivalent in full generality to<sup>19</sup>

$$\lambda = - \lim_{\varepsilon \rightarrow 0} \left. \frac{\Sigma(i\omega_n)}{i\omega_n} \right|_{n=0}, \quad (2.2)$$

where  $\varepsilon$  is the ratio between phonon frequency and the Fermi energy (we shall call it *adiabatic parameter*) and  $\Sigma(i\omega_n)$  and  $\omega_n$  are the usual self-energy and Matsubara frequencies.<sup>16,17</sup>

We are going to consider now a specific model<sup>2</sup> for the van Hove singularity of the DOS as shown in Fig. 1. This

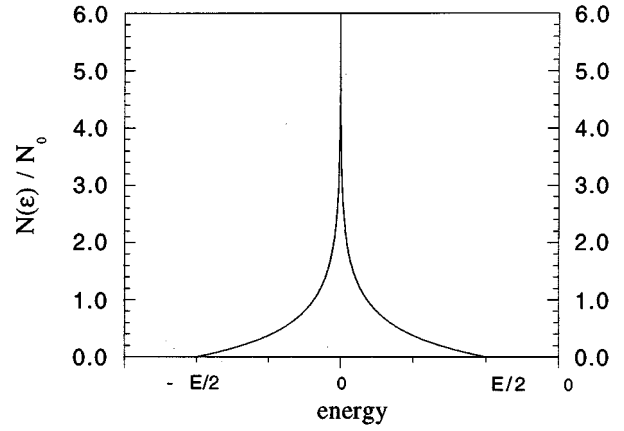


FIG. 1. Density of states corresponding to the simple model that we adopt for our calculation. This model shows a van Hove (logarithmic) singularity of the DOS. It is easy to generalize our calculations to a more realistic and complex DOS model, but the one shown here is quite representative because the critical point is the nature of the singularity.

simple model is, however, representative of all the models close to the same type of singularity.

Following Ref. 2, we use a linearization of the realistic dispersion near the saddle point

$$\epsilon(\vec{k}) = \frac{k_x k_y}{m}. \quad (2.3)$$

Here  $m$  is the effective mass and  $\vec{k}_x$  and  $\vec{k}_y$  are limited by  $|k_x|, |k_y| \leq k_c$ , where  $k_c$  represents the size of the Brillouin zone. This leads to a very simple Fermi surface made just of two lines. The total bandwidth is then

$$E = \frac{2k_c^2}{m}, \quad (2.4)$$

and the corresponding DOS is

$$N(\epsilon) = \frac{N}{2E} \int_{-k_c}^{k_c} dk_x \int_{-k_c}^{k_c} dk_y \delta(\epsilon - \epsilon(\vec{k})) = -N_0 \ln \left| \frac{2\epsilon}{E} \right|, \quad (2.5)$$

where

$$N_0 = \frac{N}{E} \quad (2.6)$$

would be the value of  $N(\epsilon)$  corresponding to a constant DOS with  $N$  states.

For a half-filling system, the Fermi level is just on the singularity  $\epsilon_F = 0$ . It should be noted that our specific model for the DOS of a two-dimensional system is actually unstable at half-filling in view of nesting effects. Our point is, however, only to focus on the role of the van Hove singularity that will be present also in stable situations. For this reason we shall not discuss any further the question of the eventual instability.

We can now derive the appropriate  $\lambda$  corresponding to our specific model assuming that the el-ph coupling is constant, e.g.,  $|g_{\vec{k},\vec{k}'}|^2 \approx g^2$ . For the self-energy, we have

$$\Sigma(i\omega_n) = -g^2 T \sum_m \frac{2\omega_0}{(\omega_n - \omega_m)^2 + \omega_0^2} \int_{-E/2}^{E/2} \frac{N(\epsilon)d\epsilon}{\epsilon - i\omega_m Z(i\omega_m)}, \tag{2.7}$$

where we consider a simple Einstein phonon.

Since the phonon propagator introduces a natural cutoff  $\omega_0$  for the frequencies, the relevant frequency values will be in a range from 0 to  $\omega_0$ . So we can approximate  $Z(i\omega_m) \approx Z_0$ . Moreover, for low temperatures we can consider the limit

$$\lim_{T \rightarrow 0} T \sum_m \rightarrow \int_{-\infty}^{\infty} \frac{d\omega}{2\pi}. \tag{2.8}$$

Then, defining  $\lambda_z$  by the relation  $Z_0 = 1 + \lambda_z$ , we obtain

$$\lambda_z = -4\lambda_0 \int_0^{E/2} \frac{d\epsilon}{Z_0} \ln\left(\frac{2\epsilon}{E}\right) \int_{-\infty}^{\infty} \frac{d\omega}{2\pi} \frac{\omega_0^2 \omega^2}{(\omega_0^2 + \omega^2)^2} \frac{1}{\omega^2 + (\epsilon/Z_0)^2}, \tag{2.9}$$

where we have used the symmetry of the band that leads also to  $\text{Re}[\Sigma(i\omega_n)] = 0$ . In addition, we have introduced

$$\lambda_0 = \frac{2g^2 N_0}{\omega_0} = \frac{2g^2 N}{\omega_0 E}, \tag{2.10}$$

which would be the value of  $\lambda$  corresponding to a constant density of states.

By performing the integrations in Eq. (2.9), we obtain

$$\lambda_z = \lambda_0 \ln\left(1 + \frac{E}{2\omega_0 Z_0}\right). \tag{2.11}$$

The energy  $E/Z_0$  represents in this approximated model the renormalized bandwidth, and our effective adiabatic parameter is

$$\varepsilon = \frac{2\omega_0 Z_0}{E}. \tag{2.12}$$

Since the effective  $\lambda$  to be taken as a reference value should be the adiabatic one [Eq. (2.2)], we finally have

$$\lambda = \lim_{\varepsilon \rightarrow 0} \lambda_z = -\lambda_0 \ln(\varepsilon). \tag{2.13}$$

This is the correct definition of the effective  $\lambda$  for a system with a singular DOS in the spirit of the phenomenological nature of Eliashberg theory.

But this is also the only theoretical definition of  $\lambda$ , both in a perturbation framework as well as in a conserving approach (i.e., Migdal's theorem). Thus the present analyses have to be performed as function of the previously defined  $\lambda$ . We expect just a small difference about the results between using  $\lambda$  or  $\lambda_0$  in the nonadiabatic regime [since  $\ln(\varepsilon)$  is of order of unity]. But we shall recover in this way also meaningful results in adiabatic limit in place of inconsistent ones obtained in function of  $\lambda_0$ .

### III. VAN HOVE SINGULARITY IN ELIASHBERG THEORY

The correct generalization of the el-ph coupling  $\lambda$ , which we have discussed in the previous section, defines the appropriate parameter to discuss the effect of singularities in the

DOS on various physical properties like, for example, the critical temperature.

A first step in this direction can be done by considering a simple "ladder" expansion for the gap equation. In the  $T$ -matrix approach, this ladder expansion can be written in the form [Fig. 2(a)]

$$\hat{T} = \hat{V} + \hat{K} \cdot \hat{T}. \tag{3.1}$$

In effect, this expansion is strictly valid in two relevant cases.

(a) Weak coupling regime ( $\lambda \ll 1$ ), but with a generical adiabatic parameter ( $\varepsilon > 1$ ). In this regime the further diagrams omitted in Fig. 2(a) can be neglected because they are of a higher order in the perturbative parameter  $\lambda$ , correctly defined by Eq. (2.13). For the same reason, using Ward's identity, we can insert the unperturbed Green functions instead of the dressed ones. This is essentially the BCS theory, recovered in the Green function framework with a retarded electron-electron interaction mediated by the phonons. For simplicity, we shall call it "retarded BCS model." In this case it is possible to generalize the theory for a generic value of  $\varepsilon$  without the need of extra diagrams.

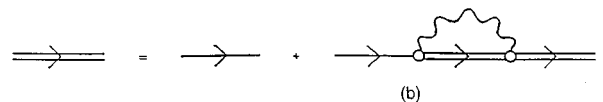
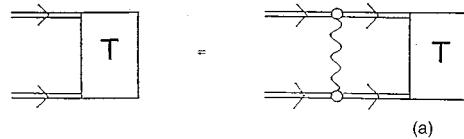


FIG. 2. (a) Diagrammatic representation for the "ladder" expansion of the  $T$  matrix. (b) Diagrammatic representation for the self-energy. In weak-coupling limit the heavy lines (renormalized Green function) in (a) can be replaced by tiny lines (bare Green propagator) and (b) becomes an identity.

(b) Adiabatic regime ( $\lambda$  generic and  $\varepsilon \ll 1$ ). In this case, for a fixed, finite value of  $\lambda$ , the neglected diagrams can be omitted because of Migdal's theorem, since they are at least of second order in  $\varepsilon$  (we shall show in Sec. IV the validity of Migdal's theorem also for a van Hove divergent density of states). The same Migdal's theorem allows us to identify the electronic self-energy with its first-order diagram [Fig. 2(b)], and so we obtain the two usual Eliashberg equations.

We would like to stress that for the correct analysis of

both these two situations a correct definition of the coupling  $\lambda$  is essential.

So, in a general way, within this ladder expansion framework, we can now write both theories as, respectively, the weak-coupling  $\lambda \rightarrow 0$  limit and adiabatic  $\varepsilon \rightarrow 0$  limit of two coupled equations: one for the self-energy and one for the superconductivity instability, shown as a diagrammatic picture in Fig. 2. The self-energy equation can be easily obtained by replacing the explicit DOS (2.5) in Eq. (2.7):

$$Z(i\omega_n) = 1 - \frac{g^2 N_0}{\omega_n} T_c \sum_m \int_{-E/2}^{E/2} \frac{d\varepsilon \ln|2\varepsilon/E|}{\omega_m^2 + [\varepsilon/Z(i\omega_m)]^2} \frac{2\omega_0 \omega_m Z(i\omega_m)}{(\omega_n - \omega_m)^2 + \omega_0^2}, \quad (3.2)$$

where we have introduced in the usual way the  $Z$  function,

$$Z(i\omega_n) = 1 - \frac{\text{Im}[\Sigma(i\omega_n)]}{i\omega_n}, \quad (3.3)$$

while the gap equation (3.1) can be written as

$$(\hat{I} - \hat{K}) \cdot \hat{T} = \hat{V}. \quad (3.4)$$

The divergence of the matrix  $\hat{T}$  for a critical temperature  $T_c$  is linked with the eigenvalue equation

$$\hat{I}\phi = \hat{K}(T_c)\phi \quad (3.5)$$

or, in explicit terms,

$$\phi(i\omega_n) = -g^2 T_c \sum_m \int \frac{d^3\vec{k}}{(2\pi)^3} D(\omega_n - \omega_m) G(\vec{k}, i\omega_m) G(-\vec{k}, -i\omega_m) \phi(i\omega_m). \quad (3.6)$$

Of course, as in standard notation,  $D$  and  $G$  are the phonon and electron Green functions. Substituting their explicit expressions in (3.6), we have

$$\phi(i\omega_n) = -g^2 T_c \sum_m \int N(\varepsilon) d\varepsilon \frac{2\omega_0}{(\omega_n - \omega_m)^2 + \omega_0^2} \frac{\phi(i\omega_m)}{[\omega_m Z(i\omega_m)]^2 + \varepsilon^2}, \quad (3.7)$$

where we have used  $\int d^2\vec{k}/(2\pi)^2 = \int N(\varepsilon) d\varepsilon$ . So, defining the gap function  $\Delta(i\omega_n) = \phi(i\omega_n)/Z(i\omega_n)$  and using our  $N(\varepsilon)$  given by Eq. (2.5), we can write

$$\Delta(i\omega_n) Z(i\omega_n) = \frac{2g^2 N_0}{\omega_0} T_c \sum_m \int_{-E/2}^{E/2} d\varepsilon \ln \left| \frac{2\varepsilon}{E} \right| \frac{\Delta(i\omega_m) Z(i\omega_m)}{[\omega_m Z(i\omega_m)]^2 + \varepsilon^2} \frac{\omega_0^2}{(\omega_n - \omega_m)^2 + \omega_0^2}. \quad (3.8)$$

Now, in order to solve in an analytic way the two coupled equations (3.2) and (3.8), we perform two main approximations.

(i) Since the intrinsic cutoff at  $\omega_0$ , given by the phonon propagator, is on  $\omega_n$  and  $\omega_m$  frequencies, the relevant values of  $Z(i\omega_n)$  in both expressions are in a range  $|\omega_n| \leq \omega_0$ . In this range, we can so approximate, as in a square-well model,  $Z(i\omega_n)$  simply by  $Z_0$  (Refs. 16, 17, 20)

$$Z(i\omega_n) \approx Z_0. \quad (3.9)$$

(ii) We simulate, in the gap equation (3.8), the effect of phonon Green function by a factorized kernel:<sup>17</sup>

$$D_{n-m} = \frac{\omega_0^2}{(\omega_n - \omega_m)^2 + \omega_0^2} \approx \frac{\omega_0^2}{\omega_n^2 + \omega_0^2} \frac{\omega_0^2}{\omega_m^2 + \omega_0^2} = D_n D_m. \quad (3.10)$$

It was shown this approximation gives the correct Combescot<sup>21</sup> prefactor ( $e$ )<sup>-1/2</sup> to  $T_c$  behavior in the constant DOS case.

Finally, we can consider the  $T_c/\omega_0 \ll 1$  limit.

According to (3.9) and (3.10), using the short notation  $\Delta_n = \Delta(i\omega_n)$ ,  $D_n = D(\omega_n)$ ,  $Z(i\omega_n) = Z_n$ , and

$$M_m = \frac{Z_0}{[\omega_m Z_0]^2 + \varepsilon^2},$$

we write Eq. (3.8) as

$$Z_0 \Delta_n = \lambda_0 T_c \sum_m \int_{-E/2}^{E/2} d\varepsilon \ln \left| \frac{2\varepsilon}{E} \right| D_n D_m M_m \Delta_m. \quad (3.11)$$

From Eq. (3.11), we can easily see the frequency behavior of  $\Delta(i\omega_n)$ :

$$\Delta(i\omega_n) = \Delta_n = \Delta_0 D_n = \Delta_0 \frac{\omega_0^2}{\omega_n^2 + \omega_0^2}. \quad (3.12)$$

By replacing Eq. (3.12) in Eq. (3.11) and dividing by  $\Delta_0$ , we have

$$Z_0 = \lambda_0 T_c \sum_m \int_{-E/2}^{E/2} d\epsilon \ln \left| \frac{2\epsilon}{E} \right| D_m^2 M_m. \quad (3.13)$$

Finally we can write, within this approximations, the two coupled equations

$$Z_0 = 1 - \frac{2\lambda_0}{\pi T_c} \int_{-\infty}^{\infty} \frac{d\omega}{2\pi} \int_0^{E/2} \frac{d\epsilon}{Z_0} \frac{\ln|2\epsilon/E|}{\omega^2 + (\epsilon/Z_0)^2} \times \frac{\omega_0^2 \omega}{\omega_0^2 + (\omega - \pi T_c)^2}, \quad (3.14)$$

$$Z_0 = 2\lambda_0 T_c \sum_m \int_0^{E/2} \frac{d\epsilon}{Z_0} \frac{\ln|2\epsilon/E|}{\omega_m^2 + (\epsilon/Z_0)^2} \frac{\omega_0^4}{(\omega_0^2 + \omega_m^2)^2} \quad (3.15)$$

[since the regular behavior of (3.14) for  $T_c/\omega_0 \rightarrow 0$ , we have calculated it for  $T=0$ ].

In weak-coupling limit (retarded BCS model), Eq. (3.14) simply states  $Z_0=1$  and Eq. (3.15) gives the usual  $T_c$  equation with a retarding factor  $\omega_0^4/(\omega_0^2 + \omega_m^2)^2$  instead of  $\theta(\omega_0 - |\omega_m|)$  of the simple BCS model. On the other hand, the adiabatic limit of Eqs. (3.14) and (3.15) corresponds to the Eliashberg theory, where (3.14) is previously calculated to give  $Z_0=1+\lambda$  and Eq. (3.15) fixes the critical temperature of this theory.

At this point, it is possible to obtain a general analytic solution of (3.14) and (3.15). The first equation, as we have seen in (2.11), gives

$$Z_0 = 1 + \lambda_0 \ln(1 + \epsilon^{-1}) = 1 - \lambda \frac{\ln(1 + \epsilon^{-1})}{\ln(\epsilon)}, \quad (3.16)$$

where we have expressed  $Z_0$  in function of our definition of  $\lambda$  and  $\epsilon$ . In a similar way, we can write Eq. (3.15) in the compact form

$$Z_0 = \frac{\lambda}{\ln(\epsilon)} I(t_c, \epsilon), \quad (3.17)$$

where  $t_c = T_c/\omega_0$  and

$$I(t_c, \epsilon) = 2T_c \sum_m \int_0^{E/2} \frac{d\epsilon}{Z_0} \frac{\ln|2\epsilon/E|}{\omega_m^2 + (\epsilon/Z_0)^2} \frac{\omega_0^4}{(\omega_0^2 + \omega_m^2)^2}. \quad (3.18)$$

Using fermionic Poisson's formula  $T \sum_m g(i\omega_m) = -\oint (dz/2\pi i) f(z)g(z)$  and introducing  $x = \epsilon/\omega_0$ , we have

$$I(t_c, \epsilon) = \int_0^{1/\epsilon} dx \ln(x\epsilon) \left[ \frac{\tanh(x/2t_c)}{x(1-x^2)^2} - \frac{1}{2(1-x^2)} - \frac{1}{(1-x^2)^2} \right]. \quad (3.19)$$

By solving Eq. (3.18) for  $t_c \ll 1$ ,

$$I(t_c, \epsilon) = -\frac{1}{2} \ln^2 \left( \frac{t_c \epsilon}{1.13} \right) + \frac{1}{2} \ln^2(\epsilon) + \frac{1}{2} \ln(1 + \epsilon^{-1}) - 0.63 - \frac{1}{4} S_1(\epsilon) - S_2(\epsilon) + \frac{1}{2} S_1(1) + 2S_2(1), \quad (3.20)$$

where  $S_1(x) = -x^2 - x^4/2^2 - x^6/3^2 - \dots$  and  $S_2(x) = x + x^3/3^2 + x^5/5^2 + \dots$ . Now, we can readily derive an analytic expression for  $T_c$  with respect to Eliashberg theory and the retarded BCS model. The first case is recovered as adiabatic limit  $\epsilon \rightarrow 0$  of Eqs. (3.16) and (3.17). The first one gives, by definition of  $\lambda$ ,

$$Z_0 = 1 + \lambda, \quad (3.21)$$

while we can easily see, by the second one,

$$Z_0 = \lambda \lim_{\epsilon \rightarrow 0} \frac{I(t_c, \epsilon)}{\ln(\epsilon)} = \lambda \left[ -\ln \left( \frac{t_c}{1.13} \right) - \frac{1}{2} \right]. \quad (3.22)$$

So  $T_c$  presents the usual expression

$$T_c = \frac{1.13}{\sqrt{e}} \omega_0 \left[ -\frac{1+\lambda}{\lambda} \right]. \quad (3.23)$$

This interesting result shows that the critical temperature is unaffected by a peak (or even a divergence) in the density of states within Eliashberg theory framework if we use the correct definition of  $\lambda$  stated by Eliashberg theory itself. *This is intrinsically due to the adiabaticity of this situation.*

In order to investigate the effect of a van Hove singularity in the nonadiabatic regime, we can consider the simple "retarded BCS" scheme. In this situation  $\lambda$  is assumed to be small while  $\epsilon$  can take any value. We have therefore, from Eq. (3.16), that

$$Z_0 = 1, \quad (3.24)$$

and Eq. (3.17) becomes

$$1 = \lambda \frac{I(t_c, \epsilon)}{\ln(\epsilon)}. \quad (3.25)$$

By using Eq. (3.20), we can finally derive the transition temperature

$$T_c = 1.13 \frac{E}{2} \exp \left[ -\sqrt{-\frac{2 \ln(\epsilon)}{\lambda} + \ln^2(\epsilon) + \ln(1 + \epsilon^{-1}) - 1.25 + f(\epsilon)} \right], \quad (3.26)$$

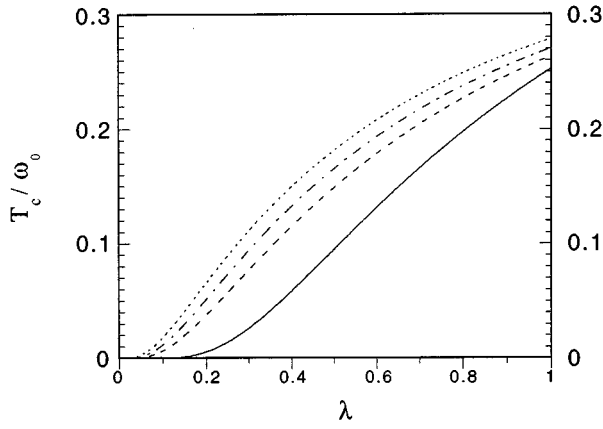


FIG. 3. Retarded BCS model.  $T_c/\omega_0$  vs coupling constant  $\lambda$  defined by Eq. (2.13) for different values of adiabatic parameter  $\varepsilon$  ( $2\omega_0/E$ ):  $\varepsilon=0$  (solid line),  $\varepsilon=0.1$  (dashed line),  $\varepsilon=0.2$  (dot-dashed line),  $\varepsilon=0.3$  (dotted line). The curve  $\varepsilon=0$  correspond to BCS behavior with the correct Combescot factor.

where, in order to simplify, we have defined  $f(\varepsilon) = -0.5S_1(\varepsilon) - 2S_2(\varepsilon) + S_1(1) + 4S_2(1)$ . The results of Eq. (3.26) are shown in Figs. 3 and 4. In Fig. 3 we can see that a nonzero value of the adiabatic parameter  $\varepsilon$  enhances the value of  $T_c$  (for a given  $\lambda$ ) with respect to the BCS reference behavior. Note that this enhancement is qualitatively different from the case in which a peak in the DOS enhances the value of  $\lambda$ . In fact, here we are comparing situations in which the value of  $\lambda$  is *fixed*, but the adiabatic parameter  $\varepsilon$  becomes different by zero.

In Fig. 4 we show the detailed behavior of  $T_c$  as a function of  $\varepsilon$  for different values of  $\lambda$ . Note that even a rather small value of  $\varepsilon$  can lead to appreciable enhancement of  $T_c$ .

It should be stressed that our results of Figs. 3 and 4 are similar to those of Refs. 2, 7, 8 for what concerns the nonadiabatic regime ( $\varepsilon \geq 0.1$ ), although the definition of  $\lambda$  is different by a factor  $-\ln(\varepsilon)$ , which in this regime is of order of unity. In order to avoid confusion, it is important to clarify this point in detail. We have separated the effect of the peak in the DOS on the actual *value* of  $\lambda$  from the effects that change the *structure* of the theory. In fact, in our approach

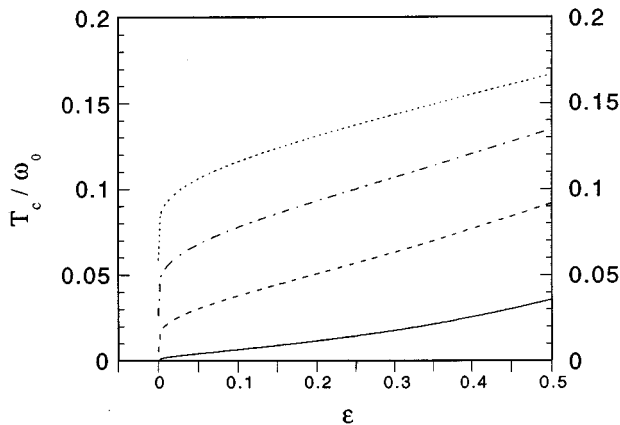


FIG. 4. Retarded BCS model. Critical temperature  $T_c/\omega_0$  in a function of the adiabatic parameter  $\varepsilon$  and different values of  $\lambda$ :  $\lambda=0.1$  (solid line),  $\lambda=0.2$  (dashed line),  $\lambda=0.3$  (dot-dashed line),  $\lambda=0.4$  (dotted line).

the BCS limit can be properly recovered as shown in Figs. 3 and 4. In Refs. 2, 7, 8 the adiabatic limit is instead problematic and the enhancement of  $T_c$  in this regime is essentially related only to the enhancement of a effective  $\delta$ .<sup>8</sup>

#### IV. VAN HOVE SINGULARITY AND VERTEX CORRECTION

In the previous section, we have considered the effect of van Hove singularities in two limiting cases that do not involve processes beyond Migdal's theorem like vertex corrections and similar effects. In previous papers<sup>14-17</sup> we have argued that there are valid reasons to expect that the high- $T_c$  SC materials do not satisfy Migdal's theorem. The possible existence of peaks in the DOS represents an additional element in this direction because the electronic energies will tend to be located in a narrow energy region. It is therefore very important and, in some sense unavoidable, to consider processes beyond Migdal's theorem when dealing with peaks in the DOS. For these reasons we shall now consider in some detail the effect of a van Hove peak in the DOS on the vertex correction diagrams as shown in Fig. 5. Such vertex corrections appear in the theory through the vertex function defined by (Fig. 5)

$$P(\omega_n, \omega_m, \vec{q}; \omega_0, E) = \frac{2g^2}{\omega_0} T \sum_l \int \frac{d^2k}{(2\pi)^2} \frac{\omega_0^2}{\omega_0^2 + (\omega_l - \omega_n)^2} \times \frac{1}{i\omega_l - \epsilon(\vec{k})} \times \frac{1}{i\omega_m + i\omega_l - i\omega_n - \epsilon(\vec{k} + \vec{q})}. \quad (4.1)$$

It was noted that the relevant dependence of  $P(\omega_n, \omega_m, \vec{q}; \omega_0, E)$  is through the difference  $\omega_n - \omega_m$ .<sup>17</sup> In order to focus our interest on this dependence, we put an electronic frequency to zero  $\omega_n = 0$ . In such a way,  $\omega_m$  will represent the exchanged phonon frequency. Then Eq. (4.1) becomes

$$P(\omega_m, \vec{q}; \omega_0, E) = \frac{2g^2}{\omega_0} T \sum_l \int \frac{d^2k}{(2\pi)^2} \frac{\omega_0^2}{\omega_0^2 + \omega_l^2} \frac{1}{i\omega_l - \epsilon(\vec{k})} \times \frac{1}{(i\omega_m + i\omega_l) - \epsilon(\vec{k} + \vec{q})}. \quad (4.2)$$

Following Ref. 16, we can perform the sum on  $\omega_l$  in the zero-temperature limit. We obtain

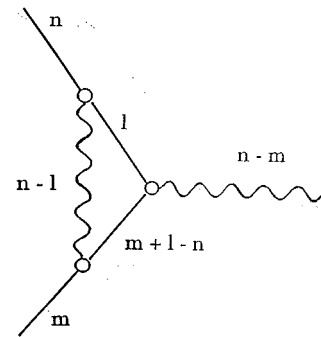


FIG. 5. First-order vertex correction diagram.

$$\begin{aligned}
P(\omega, \vec{q}; \omega_0, E) &= \frac{g^2}{i} \int \frac{d^2k}{(2\pi)^2} \frac{1}{\omega + i[\epsilon(\vec{k}) - \epsilon(\vec{k} + \vec{q})]} \\
&\times \left[ \frac{\theta(\epsilon(\vec{k}))}{\omega_0 + \epsilon(\vec{k})} - \frac{\theta(-\epsilon(\vec{k}))}{\omega_0 - \epsilon(\vec{k})} \right. \\
&+ \frac{i\theta(\epsilon(\vec{k} + \vec{q}))}{\omega - i[\omega_0 + \epsilon(\vec{k})]} \\
&\left. + \frac{i\theta(-\epsilon(\vec{k} + \vec{q}))}{\omega + i[\omega_0 - \epsilon(\vec{k} + \vec{q})]} \right]. \quad (4.3)
\end{aligned}$$

So far, these expressions are quite general. Now, in order to introduce explicitly the van Hove singularity, we need to specify the energy dispersion  $\epsilon(\vec{k})$ . We use the electronic band (2.3), and so we shall directly evaluate the effect of vertex corrections on the previous ladder results.

Before going on with a derivation of the complex  $(\omega - \vec{q})$  dependence of  $P(\omega, \vec{q}; \omega_0, E)$ , we would like to consider two particular limits of this function: the *dynamical* and *static* ones. The first one simply states, by a well-known Ward's identity,

$$P_d = \lim_{\omega \rightarrow 0} \lim_{\vec{q} \rightarrow 0} P(\omega, \vec{q}; \omega_0, E) = \lambda_0 \ln(1 + \epsilon^{-1}). \quad (4.4)$$

Note that the adiabatic limit of  $P_d$  is one of the theoretical definition of  $\lambda$  and is coincident with our definition. About the static limit  $P_s$ , it is immediately shown that

$$P_s = \lim_{\vec{q} \rightarrow 0} \lim_{\omega \rightarrow 0} P(\omega, \vec{q}; \omega_0, E) = -\infty. \quad (4.5)$$

This is an unavoidable divergence strictly connected with the singularity in the DOS. It shows that a system with a Fermi level close a van Hove singularity is automatically near a  $\vec{q}$ -zero instability (phase separation). Anyway, this two limits show a complex dependence on  $\omega - \vec{q}$  variables.

Now, given these results, we are going to consider  $P(\omega, \vec{q}; \omega_0, E)$  in more detail. In order to obtain an analytical expression for vertex function, we perform a drastic approximation on the energy dispersion: Keeping fixed the logarithmic divergent DOS given by Eq. (2.5), we assume the Fermi surface be isotropic (therefore spherical). This assumption is clearly inconsistent with the presence of a saddle point at  $\epsilon = \epsilon_F$ . However, we shall see the main effect of the saddle point is not given by its anisotropy, but is given by the singularity connected with it. In effect, the results obtained from this model show a good agreement in comparison with those ones derived by correct numerical calculations.

Note that the logarithmic divergence given by the DOS intrinsically selects states close Fermi energy. It is therefore a good approximation expanding  $\epsilon(\vec{k} + \vec{q})$  for small  $\vec{q}$ :

$$\epsilon(\vec{k} + \vec{q}) \approx \epsilon(\vec{k}) + v_{\vec{F}} \cdot \vec{q} = \epsilon(\vec{k}) + v_{\vec{F}} q \sin\left(\frac{\alpha}{2}\right), \quad (4.6)$$

where  $\alpha$  is the angle between  $\vec{k}$  and  $\vec{k} + \vec{q}$ . Using  $\int d^2k/(2\pi)^2 = \int N(\epsilon) d\epsilon \int_{-\pi}^{\pi} d\alpha/2\pi$ , we can easy see that the first two terms of Eq. (4.3) will cancel by symmetry. Then, denoting  $y = v_{\vec{F}} q \sin(\alpha/2)$ ,  $Q = q/2k_F$ ,  $E = 2E_F = 2v_{\vec{F}}k_F$ , we can rewrite Eq. (4.3) as

$$P(\omega, Q; \omega_0, E) = -\lambda_0 \frac{\omega_0}{4EQ} \int_{-EQ}^{EQ} \frac{dy}{\omega^2 + y^2} \int_{-E/2}^{E/2} d\epsilon \ln \left| \frac{2\epsilon}{E} \left[ \theta(\epsilon - y) \frac{y(\omega_0 + \epsilon - y) + \omega^2}{\omega^2 + (\omega_0 + \epsilon - y)^2} + \theta(y - \epsilon) \frac{y(\omega_0 + y - \epsilon) + \omega^2}{\omega^2 + (\omega_0 + y - \epsilon)^2} \right] \right|, \quad (4.7)$$

where, for the same reasons of Eq. (4.6), we have put  $d\alpha \approx 2d \sin(\alpha/2)$ . By a change of variables  $\epsilon \rightarrow -\epsilon$ ,  $y \rightarrow -y$ , we can rewrite Eq. (4.7) as

$$P(\omega, Q; \omega_0, E) = -\lambda_0 \frac{\omega_0}{2EQ} \int_{-EQ}^{EQ} \frac{dy}{\omega^2 + y^2} \int_y^{E/2} d\epsilon \ln \left| \frac{2\epsilon}{E} \frac{y(\omega_0 + \epsilon - y) + \omega^2}{\omega^2 + (\omega_0 + \epsilon - y)^2} \right|, \quad (4.8)$$

or, in other terms,

$$P(\omega, Q; \omega_0, E) = \lambda_0 \frac{\omega_0}{2EQ} \int_{-EQ}^{EQ} \frac{dy}{\omega^2 + y^2} [yF_a(y) + F_b(y)], \quad (4.9)$$

where we define

$$F_a(y) = - \int_y^{E/2} d\epsilon \frac{\ln|2\epsilon/E|(\omega_0 + \epsilon - y)}{\omega^2 + (\omega_0 + \epsilon - y)^2}, \quad (4.10)$$

$$F_b(y) = - \omega^2 \int_y^{E/2} d\epsilon \frac{\ln|2\epsilon/E|}{\omega^2 + (\omega_0 + \epsilon - y)^2}. \quad (4.11)$$

The main contribute of  $F_a(y)$  and  $F_b(y)$  corresponds to small values of  $y$  because the logarithmic term. We can so expand them for  $y \rightarrow 0$ :

$$F_a(y) \approx \lim_{y \rightarrow 0} F_a(y) + y \lim_{y \rightarrow 0} F'_d(y), \quad (4.12)$$

$$F_b(y) \simeq \lim_{y \rightarrow 0} F_b(y) + y \lim_{y \rightarrow 0} F'_b(y) + \frac{y^2}{2} \lim_{y \rightarrow 0} F''_b(y). \quad (4.13)$$

The only terms in Eq. (4.9) that can be a nonzero contribute after their integration are the even ones. So we can reduce Eq. (4.9):

$$P(\omega, Q; \omega_0, E) = \lambda_0 \frac{\omega_0}{2EQ} \int_{-EQ}^{EQ} \frac{dy}{\omega^2 + y^2} \left\{ \lim_{y \rightarrow 0} F_b(y) + y^2 \left[ \lim_{y \rightarrow 0} F'_a(y) + \frac{1}{2} \lim_{y \rightarrow 0} F''_b(y) \right] \right\}. \quad (4.14)$$

The first limit is regular in  $y=0$  and gives, in the limit  $\omega \ll E/2$ ,

$$\lim_{y \rightarrow 0} F_b(y) = F_b(0) = \omega \ln \left( \frac{E}{2\omega_0} \right) \arctan \left( \frac{\omega}{\omega_0} \right) + \frac{\omega^2}{\omega_0} \ln \left( 1 + \frac{2\omega_0}{E} \right). \quad (4.15)$$

The other contributes need more care. With regard to  $F'_a(y)$ , as a first step we divide  $F_a(y)$  by writing  $\ln|2\epsilon/E| = \ln|2y/E| + \ln|\epsilon/y|$ . Then,

$$F_a(y) = F_{a1}(y) + F_{a2}(y) = - \ln \left| \frac{2y}{E} \right| \int_y^{E/2} d\epsilon \frac{(\omega_0 + \epsilon - y)}{\omega^2 + (\omega_0 + \epsilon - y)^2} - \int_y^{E/2} d\epsilon \frac{\ln|\epsilon/y|(\omega_0 + \epsilon - y)}{\omega^2 + (\omega_0 + \epsilon - y)^2}. \quad (4.16)$$

Expanding the first term for small  $y$ , we have

$$\lim_{y \rightarrow 0} F'_{a1}(y) = \ln \left| \frac{2y}{E} \right| \frac{(\omega_0 + E/2)}{\omega^2 + (\omega_0 + E/2)^2}, \quad (4.17)$$

while we can see that the second term, for  $y \rightarrow 0$ , is even in  $y$ . So it will give an odd function in the integral, and its contribution will be zero. Thus we simply have  $F_a(y) = F'_{a1}(y)$ . The same procedure can be applied to  $F''_b(y)$ , with an opposite-parity selection, of course. We obtain

$$\lim_{y \rightarrow 0} F''_b(y) = \ln \left| \frac{2y}{E} \right| \frac{2\omega^2(\omega_0 + E/2)}{[\omega^2 + (\omega_0 + E/2)^2]^2}. \quad (4.18)$$

We can summarize this result in the expression

$$P(\omega, Q; \omega_0, E) = \lambda_0 \frac{\omega_0}{2EQ} \int_{-EQ}^{EQ} \frac{dy}{\omega^2 + y^2} [A(\omega) + B(\omega)y^2 \ln(2y/E)], \quad (4.19)$$

where

$$A(\omega) = \omega \ln \left( \frac{E}{2\omega_0} \right) \arctan \left( \frac{\omega}{\omega_0} \right) + \frac{\omega^2}{\omega_0} \ln \left( 1 + \frac{2\omega_0}{E} \right), \quad (4.20)$$

$$B(\omega) = (\omega_0 + E/2) \frac{2\omega^2 + (\omega_0 + E/2)^2}{[\omega^2 + (\omega_0 + E/2)^2]^2}. \quad (4.21)$$

Finally, we can perform the last integral on  $y$ , and we obtain the final result

$$\begin{aligned} P(\omega, Q; \omega_0, E) &= \left( \frac{\omega_0}{EQ} \right) \arctan \left( \frac{EQ}{\omega} \right) \left[ -\omega \int_0^{E/2} \frac{d\epsilon \ln|\epsilon/E|}{\omega^2 + (\omega_0 + \epsilon)^2} \right] + \omega_0(\omega_0 + E/2) \frac{2\omega^2 + (\omega_0 + E/2)^2}{[\omega^2 + (\omega_0 + E/2)^2]^2} [\ln(2Q) - 1] \\ &\quad - \omega_0(\omega_0 + E/2) \frac{2\omega^2 + (\omega_0 + E/2)^2}{[\omega^2 + (\omega_0 + E/2)^2]^2} \left( \frac{\omega}{EQ} \right) \arctan \left( \frac{EQ}{\omega} \right) \ln(2Q) \\ &\quad + \omega_0(\omega_0 + E/2) \frac{2\omega^2 + (\omega_0 + E/2)^2}{[\omega^2 + (\omega_0 + E/2)^2]^2} \left( \frac{\omega}{EQ} \right) \frac{1}{2} \int_{-EQ/\omega}^{EQ/\omega} \frac{dz}{z} \arctan(z). \end{aligned} \quad (4.22)$$

The two integrals in Eq. (4.22) have no analytic expression. We recall their main limits

$$-\omega \int_0^{E/2} \frac{d\epsilon \ln|2\epsilon/E|}{\omega^2 + (\omega_0 + \epsilon)^2} = \ln \left( \frac{E}{2\omega_0} \right) \arctan \left( \frac{\omega}{\omega_0} \right) + \begin{cases} \frac{\omega}{\omega_0} \ln \left( 1 + \frac{E}{2\omega_0} \right), & \frac{E}{2\omega} \gg 1, \\ \frac{\omega_0}{\omega} \left[ 1 + \frac{2}{\omega_0} + \ln \left( \frac{2}{\omega_0} \right) \right], & \frac{E}{2\omega} \ll 1, \end{cases} \quad (4.23)$$

$$\frac{1}{2} \int_{-EQ/\omega}^{EQ/\omega} \frac{dz}{z} \arctan(z) = \begin{cases} \frac{EQ}{\omega}, & \frac{EQ}{\omega} \ll 1, \\ \frac{\pi}{2} \ln \left| \frac{EQ}{\omega} \right|, & \frac{EQ}{\omega} \gg 1. \end{cases} \quad (4.24)$$

The expression in Eq. (4.22) represents the direct extension of the vertex calculations of Refs. 14–17 in the case of a van Hove singular density of states. As in these papers, the vertex function  $P(\omega, Q; \omega_0, E)$  shows a nontrivial dependence of momentum and frequency variables. An example of the detailed behavior of  $P(\omega, Q; \omega_0, E)$  versus frequency at various fixed momentum  $Q$  is plotted in Fig. 6, while its sign is shown in Fig. 7. As one can see, the regions of positivity and negativity are close, respectively, to the dynamical and static limits of it. From a general point of view, we expect that a physical selection of small  $q$  will correspond to a positive vertex corrections as in Refs. 15–17.

We would like also to compare the present result with a numerical analysis of vertex function beyond the approximation (4.6). In this perspective we have performed the integral in Eq. (4.3) in a numerical way by using, for a correct com-

parison, the anisotropic energy distribution (2.3). Of course, unlike the previous isotropic model, we have now an explicit dependence on the direction of  $\vec{q}$ . To make a qualitative comparison, we choose the simple case  $\vec{q} = (q, q)$ . It gives representative results of a generical vector  $\vec{q}$ , but we would not give a quantitative relevance to this comparison. However, Figs. 6 and 7 show a good agreement between the analytic and numerical results in spite of the substantial differences of the two approaches, in particular in the region of *small* momenta.

As a direct application of the present analytic calculations, we can now prove the validity of Migdal’s theorem in the case of a van Hove singularity. Performing the adiabatic limit  $2\omega_0/E \ll 1$  in Eq. (4.22) at *fixed*  $\omega$  and  $Q$ , we easily obtain

$$\lim_{\varepsilon \rightarrow 0} P(\omega, Q; \omega_0, E) = \lambda_0 \frac{\pi}{4Q} \arctan\left(\frac{\omega}{\omega_0}\right) \ln\left(\frac{E}{2\omega_0}\right) \approx \lambda \varepsilon. \quad (4.25)$$

The logarithmic factor in Eq. (4.25) was usually interpreted as a weakening of Migdal’s theorem validity,<sup>12,22</sup> so that this theorem could be applied just with the accuracy of order  $\varepsilon \ln(\varepsilon)$ . On the other hand, as we can easily see in the same Eq. (4.25), this problem is nonexistent with a correct definition of the coupling constant on which Migdal’s theorem is based. So the apparent weakness of Migdal’s theorem is rather a signal that a “good” definition of  $\lambda$  is necessary.

### V. $T_c$ WITH VAN HOVE SINGULARITY BEYOND MIGDAL’S THEOREM

In the previous section, we have examined in some detail, for a system with a van Hove singularity at Fermi level, the general behavior of the vertex function  $P(\omega, \vec{q}; \omega_0, E)$  versus momentum and frequency of the exchanged phonon.

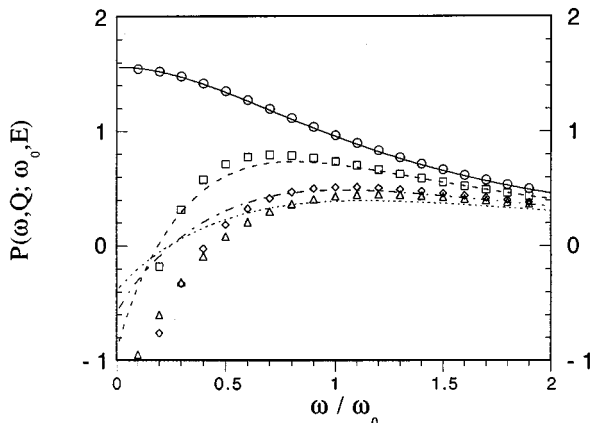


FIG. 6. Behavior of analytic  $P(\omega, Q; \omega_0, E)$  (curves) vs  $\omega$  in comparison with a numerical approach (points) for different values of  $Q$ :  $Q=0$  (solid line, circles),  $Q=0.2$  (dashed line, squares),  $Q=0.4$  (dot-dashed line, diamonds),  $Q=0.6$  (dotted line, triangles).

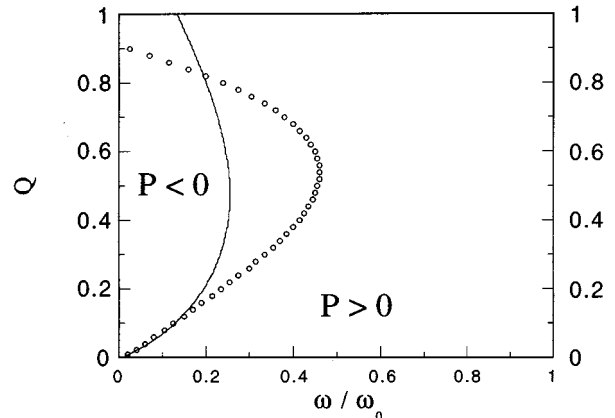


FIG. 7. Sign of the analytic vertex function  $P(\omega, Q; \omega_0, E)$  [Eq. (4.22)] in  $Q$ - $\omega$  space ( $Q = q/2k_F$ ). The solid line represents the curve  $P(\omega, Q; \omega_0, E) = 0$ . On the left side the function is negative, while on the other side it is positive. We also plot the same quantity according to a numerical calculation using the dispersion (2.3) (see text). In this case,  $Q = q/k_c$ .

In this section we would like to apply this result in order to investigate the effects of the first vertex corrections on the determination of the critical temperature. In this perspective we are going to insert explicitly the contribute of vertex (and cross) corrections in the framework of a generalization of the

Eliashberg equation<sup>17</sup> at the first order beyond Migdal's theorem. The respective corrections with respect to the two equations are shown in the diagrammatic picture in Fig. 8. In particular, the phonon-mediated electron-electron interaction becomes, for the self-energy equation,

$$g^2 D(\omega_n - \omega_m) \rightarrow \tilde{V}_{n,m}^Z(\vec{p} - \vec{k}) = g^2 \left[ D(\omega_n - \omega_m) + \lambda_0 D(\omega_n - \omega_m) \sum_{\vec{k}'} T \sum_l G(\vec{k}', i\omega_l) G(\vec{k}' + \vec{p} - \vec{k}, i\omega_l + i\omega_m - i\omega_n) \right. \\ \left. \times D(\omega_n - \omega_l) \right], \quad (5.1)$$

and, for the gap equation,

$$g^2 D(\omega_n - \omega_m) \rightarrow \tilde{V}_{n,m}^\Delta(\vec{p} - \vec{k}) = g^2 \left[ D(\omega_n - \omega_m) + 2\lambda_0 D(\omega_n - \omega_m) \sum_{\vec{k}'} T \sum_l G(\vec{k}', i\omega_l) G(\vec{k}' + \vec{k} - \vec{p}, i\omega_l + i\omega_m - i\omega_n) \right. \\ \left. \times D(\omega_n - \omega_l) + \lambda_0 \sum_{\vec{k}'} T \sum_l D(\omega_n - \omega_l) D(\omega_l - \omega_m) G(\vec{k}', i\omega_l) G(\vec{k}' + \vec{k} - \vec{p}, i\omega_l + i\omega_m - i\omega_n) \right]. \quad (5.2)$$

Equation (5.1) can be easily written as

$$\tilde{V}_{n,m}^Z(\vec{p} - \vec{k}) = g^2 D(\omega_n - \omega_m) [1 + P(\omega_n, \omega_m, \vec{p} - \vec{k}; \omega_0, E)], \quad (5.3)$$

while in Eq. (5.2) the product  $D_{n-l} D_{l-m}$  due to the cross factor can be approximated<sup>17</sup> by  $D_{n-m} D_{n-l}$  in the region of reasonable frequencies. Then we can so draw the corresponding interaction for the gap equation in a similar form as Eq. (5.3):

$$\tilde{V}_{n,m}^\Delta(\vec{p} - \vec{k}) = g^2 D(\omega_n - \omega_m) [1 + 2P(\omega_n, \omega_m, \vec{p} - \vec{k}; \omega_0, E) + P(\omega_n, \omega_m, \vec{p} + \vec{k}; \omega_0, E)]. \quad (5.4)$$

The two new equations obtained by using these corrected interactions are too complex to handle in a simple way. It is necessary for performing further approximations. The first one is the usual average on the Fermi surface. In this way we neglect, for the moment, the explicit momenta dependence of vertex and cross contribution:

$$\tilde{V}_{n,m}^Z(\vec{p} - \vec{k}) \rightarrow \langle \langle \tilde{V}_{n,m}^Z(\vec{p} - \vec{k}) \rangle \rangle_{\text{FS}}, \\ g^2 P(\omega_n, \omega_m, \vec{p} - \vec{k}; \omega_0, E) \rightarrow \langle \langle g^2 P(\omega_n, \omega_m, \vec{p} - \vec{k}; \omega_0, E) \rangle \rangle_{\text{FS}}, \\ g^2 P(\omega_n, \omega_m, \vec{p} + \vec{k}; \omega_0, E) \rightarrow \langle \langle g^2 P(\omega_n, \omega_m, \vec{p} + \vec{k}; \omega_0, E) \rangle \rangle_{\text{FS}}$$

(we include the matrix element in the average in order to extend, in a next step, our analysis to the case of a momenta dependence of  $g$ ). In the same spirit of a Fermi surface average, we would like to apply a similar procedure to the vertex and cross with respect to the dependence on frequencies. In particular, we could substitute them with a weighted average on the two frequencies  $\omega_n$  and  $\omega_m$  using a weight  $p_i = \omega_i^2 / (\omega_0^2 + \omega_i^2)$  to simulate the effect of the phonon propagator. Since the vertex and cross depend essentially on the frequency difference, we put  $\omega_n = 0$  and perform the weighted average only on  $\omega_m$ . Explicitly,

$$g^2 P_{v/c}(\varepsilon) = \frac{\sum_m \frac{\omega_0^2}{(\omega_0^2 + \omega_m^2)} \langle \langle g^2 P(\omega_n = 0, \omega_m, \vec{p} \mp \vec{k}; \omega_0, E) \rangle \rangle_{\text{FS}}}{\sum_m \frac{\omega_0^2}{(\omega_0^2 + \omega_m^2)}}. \quad (5.5)$$

After these manipulations we can eventually draw the new equations of the generalized Eliashberg theory at first order beyond Migdal's theorem:

$$Z_n = 1 - \tilde{\lambda}_0^Z T_c \sum_m \frac{\omega_m}{\omega_n} \int_{-E/2}^{E/2} d\varepsilon \ln \left| \frac{2\varepsilon}{E} \right| M_m D_{n-m} Z_m, \quad (5.6)$$

$$\Delta_n Z_n = \tilde{\lambda}_0^\Delta T_c \sum_m \int_{-E/2}^{E/2} d\varepsilon \ln \left| \frac{2\varepsilon}{E} \right| M_m D_{n-m} \Delta_m Z_m, \quad (5.7)$$

where

$$\tilde{\lambda}_0^Z = \lambda_0 [1 + P_v(\varepsilon)] \equiv - \frac{\tilde{\lambda}^Z}{\ln(\varepsilon)}, \tag{5.8}$$

$$\tilde{\lambda}_0^\Delta = \lambda_0 [1 + 2P_v(\varepsilon) + P_c(\varepsilon)] \equiv - \frac{\tilde{\lambda}^\Delta}{\ln(\varepsilon)}. \tag{5.9}$$

Equations (5.8) and (5.9) are formally identical to the classic Eliashberg equations that we have previously solved in an approximated analytic way. In the same context, we can therefore generalize Eqs. (3.23), (3.26) to include first-order vertex and cross corrections:

$$T_c = 1.13 \frac{E}{2} \exp \left[ - \sqrt{ - \frac{2\tilde{Z}_0 \ln(\varepsilon)}{\tilde{\lambda}^\Delta} + \ln^2(\varepsilon) + \ln(1 + \varepsilon^{-1}) - 1.25 + f(\varepsilon) } \right], \tag{5.10}$$

where

$$\tilde{Z}_0 = 1 - \tilde{\lambda}^Z \ln(1 + \varepsilon^{-1}) / \ln(\varepsilon). \tag{5.11}$$

In these expressions  $\tilde{\lambda}^Z$  and  $\tilde{\lambda}^\Delta$  depend themselves on  $\lambda$  and  $\varepsilon$ . Now, in order to get a numerical value of the critical temperature by Eq. (5.10), we have to explicit the effective coupling constants  $\tilde{\lambda}^Z$  and  $\tilde{\lambda}^\Delta$  or, in other words, to perform the average procedures. In particular, we focus our attention on the average on Fermi surface.

In the previous section, in fact, we have argued, as in the case of a flat band, a positive contribute of the vertex corrections in the small exchanged momenta region. On the other hand, we expect that, in the present case, these momenta are the most relevant because of the logarithmic divergence in the density of states.

Thus, in order to investigate the relative dependence of the critical temperature  $T_c$  on a particular region of  $q$  space, we include the first-order corrections beyond Migdal's theorem in function of a parameter  $Q_c$ , which represents a cutoff selection of momenta  $q$ . We shall follow essentially the procedure of Ref. 17, applying it to the present system. In particular, we introduce a nonconstant matrix element

$$|g_{\vec{k}, \vec{p}}|^2 = g^2 \frac{\theta(q_c - |\vec{p} - \vec{k}|)}{\langle \langle \theta(q_c - |\vec{p} - \vec{k}|) \rangle \rangle_{\vec{p}, \vec{k} \in \text{FS}}}, \tag{5.12}$$

where we have normalized it in order to recover the fixed experimental  $\lambda$  in the adiabatic limit for any parameter  $q_c$ .

In this way the averages on the Fermi surface turn out to depend on, besides  $\varepsilon$ , a parameter  $q_c$ . By varying it we can probe the specific relevance of different momenta regions. The average of the vertex correction (4.22) does not present particular difficulties, because the cutoff works just on the variable  $Q = |\vec{p} - \vec{k}|/2k_F$ . Unfortunately, the average of the cross contribution cannot directly calculated in the same way because in this case it is a function of  $k + \vec{p}$  so that that the cutoff condition on the vector  $k - \vec{p}$  is not easily related to the vector  $k + \vec{p}$ . However, we can make some considerations connected with the particular geometry of the real Fermi surface. In fact, as one can see from Fig. 9, for the Fermi surface of dispersion (2.3) a cutoff  $q_c$  on  $k - \vec{p}$  gives the same cutoff on the vector  $k + \vec{p}$ . In this case the average of the cross term is equal to the vertex one. This argument is quite general, and it is only related to the linearization of the Fermi surface near the saddle point. So it is valid for any Fermi

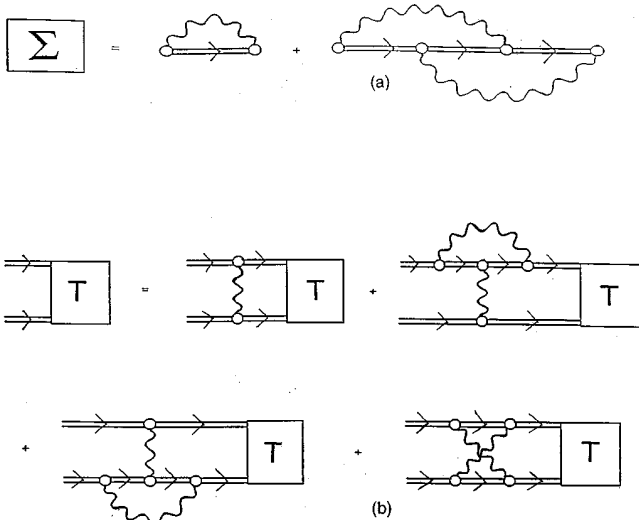


FIG. 8. First corrections beyond Migdal's theorem for self-energy and gap equations.

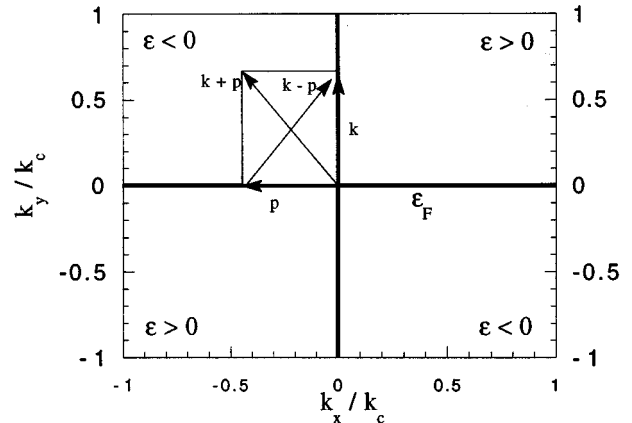


FIG. 9. For the electronic dispersion (2.3), a momenta selection of  $|\vec{k} - \vec{p}|$  at  $q_c$  (with  $\vec{k}$  and  $\vec{p}$  lying on Fermi surface) corresponds to same selection on  $|\vec{k} + \vec{p}|$ . This result is not strictly related to the particular Fermi surface, but it is verified for any linearization of the Fermi surface near the saddle point, that is, the region of small  $q_c$ .

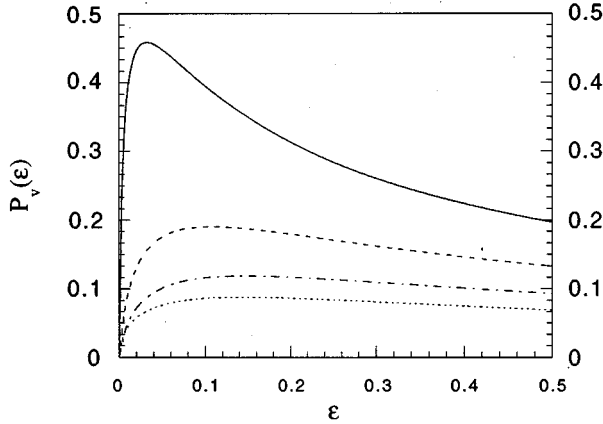


FIG. 10. Momentum and frequency averages of the vertex contribution  $P_v(\epsilon)$  plotted vs the adiabatic parameter  $\epsilon$  for  $\lambda_0 = 0.3$ . The different curves correspond to  $Q_c = 0.05$  (solid line),  $Q_c = 0.25$  (dashed line),  $Q_c = 0.45$  (dot-dashed line),  $Q_c = 0.65$  (dotted line).

surface and for any  $\vec{k}, \vec{p}$  enough close to the saddle point. As we are interested just in this region of momenta, we can assume that the contribution of the cross correction is equal to the vertex correction.

As a result of the selected average on the Fermi surface, we obtain then a dependence of  $P_v(=P_c)$  on a further parameter  $Q_c$ :

$$P_v(\epsilon) = P_c(\epsilon) = P_v(\epsilon, Q_c). \quad (5.13)$$

The behavior of  $P_v(\epsilon, Q_c)$  versus the adiabatic parameter  $\epsilon$  for different value of  $Q_c$  is shown in Fig. 10. It is qualitatively similar to the constant DOS case.<sup>17</sup>

We can now evaluate the effect of the first vertex and cross corrections on the critical temperature as function of the parameters  $\lambda$ ,  $\epsilon$ , and  $Q_c$  [ $T_c = T_c(\epsilon)$ ]. From Figs. 11 and 12, we can see that these corrections give substantially an enhancement of  $T_c$ , and this enhancement is as more marked as the momenta selection is restricted. Thus the effect of vertex corrections for an opportune selection can even lead to a factor of 2 to the value of the critical temperature. Anyway, it should be stressed the basic increase of  $T_c$  with respect of Migdal-Eliashberg theory is given by the simple nonadiabatic expression (3.26) also in the strong-coupling regime without vertex corrections in spite of the large contribute of them for small  $Q_c$ . This result can be read as evidence of the automatic selection in the momenta region due to the logarithmic singularity. In this case is clear that a further cutoff on this region can just amplify the effects of vertex corrections, but they are not necessary to recover a high  $T_c$ . To make a direct comparison among the different approaches, we show in Table I the critical temperature for the respective theories.

## VI. CONCLUSIONS

In this paper we have analyzed the role of the nonadiabaticity in the context of a van Hove scenario applied to superconductivity. A first crucial step is the identification of the coupling constant  $\lambda$ . By a general definition of it, we have identified  $\lambda$  for a system with a logarithmic singularity (van

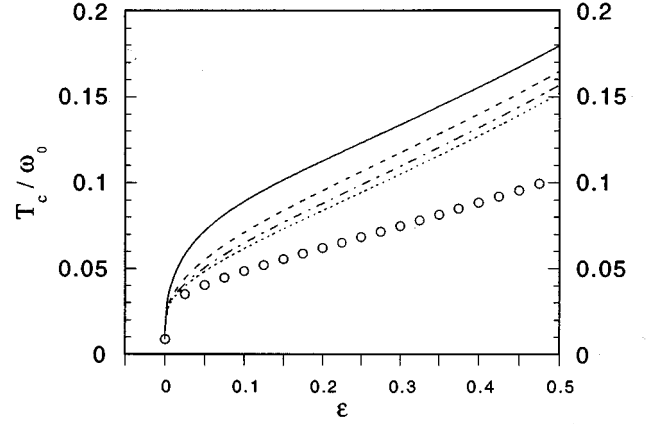


FIG. 11. Behavior of the critical temperature  $T_c$  [Eq. (5.10)] of generalized Eliashberg equations to include first corrections beyond Migdal's theorem. We plot  $T_c$  as function of  $\epsilon$  for  $\lambda = 0.3$  and different values of  $Q_c$ :  $Q_c = 0.05$  (solid line),  $Q_c = 0.25$  (dashed line),  $Q_c = 0.45$  (dot-dashed line),  $Q_c = 0.65$  (dotted line). These curves are compare with the behavior of  $T_c$  obtained by the same calculations without including vertex and cross corrections (circles).

Hove-singularity) in the density of states. We have shown this definition allows us to go from a classic (low) critical temperature to a van Hove (high) behavior of  $T_c$  by varying the adiabatic parameter  $\epsilon = \omega_0/E_F$ . Another question due to the nonadiabaticity is the evaluation of the corrections to Migdal's theorem (vertex and cross). Using an isotropic model with a van Hove DOS, we have performed an analytic calculation of the vertex diagram in the function of momentum and frequency ( $\omega - q$ ) of the exchanged phonon. The adiabatic validity of Migdal's theorem for such a system is recovered at the same order of the usual flat DOS system. Moreover, we obtain a complex structure of vertex function versus  $\omega$  and  $q$  where the region of small exchanged momenta gives essentially a positive contribute. Finally, we

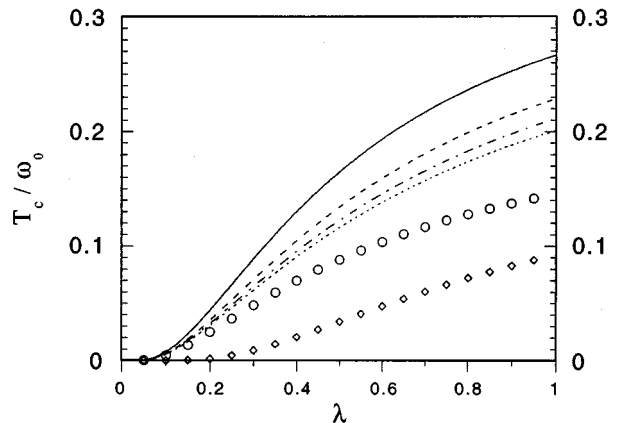


FIG. 12.  $T_c$  vs  $\lambda$  of generalized Eliashberg equations with vertex corrections at fixed  $\epsilon = 0.1$  and for different  $Q_c$ :  $Q_c = 0.05$  (solid line),  $Q_c = 0.25$  (dashed line),  $Q_c = 0.45$  (dot-dashed line),  $Q_c = 0.65$  (dotted line). The circles correspond to the same theory without vertex and cross corrections and the diamonds to the adiabatic behavior (Migdal-Eliashberg).

TABLE I. Comparison among the critical temperatures  $T_c$  of a system with a van Hove singularity obtained from different approaches: Migdal-Eliashberg theory (adiabatic limit), retarded BCS model, nonadiabatic strong-coupling model (without vertex corrections), Eliashberg theory generalization to include vertex and cross correction with a cutoff on exchanged momenta, respectively,  $Q_c=0.65$  and  $Q_c=0.05$ . The parameter choice is  $\lambda=0.3$  and  $\omega_0=1000$  K. We point out the drastic increase of  $T_c$  in the nonadiabatic region (also with small  $\epsilon$ ) for any approach.

	$\epsilon$	$T_c$ (K)
Migdal-Eliashberg	0	9
Retarded BCS	0.1	77
Strong coupling	0.1	48
Vertex $Q_c=0.65$	0.1	62
Vertex $Q_c=0.05$	0.1	89

have included these corrections beyond Migdal's theorem in a simplified generalization of Eliashberg equations with a further parameter  $Q_c$  which represents a physical selection of small momenta. The effect of these corrections on  $T_c$  results

in being an enhancement more marked as relevant momenta are small. We would like to conclude, underlining some points we have not discussed. The first is the smearing of the singularity due to the disorder and to the three-dimensional structure of the real materials can invalidate this model. About this point there are now many papers pointing out that this effect should be negligible (see, for example, Ref. 23). In any case in our perspective the divergence in the DOS is not essential and similar qualitative results can be recovered also with a sharp, but not divergent, peak in the DOS.

Besides, we would like to stress that our analyses focus on the singularity in the density of states. This characteristic can explain some features of layered superconducting materials as a high  $T_c$  or small isotopic effect. There are, however, many other properties due to the peculiar geometry of the Fermi surface close to the saddle point (for example, we have not investigated the possibility of anisotropic superconductivity which can be favored or not by the saddle point<sup>4,18</sup>). In effect, it is worth remembering, as some authors have shown, that a Fermi level near the saddle point can lead to marginal Fermi liquid properties and to linear behavior of the resistivity<sup>24,28</sup> or a short coherence length.<sup>2,25</sup>

- <sup>1</sup>J. Labbé, S. Barisic, and J. Friedel, Phys. Rev. Lett. **19**, 1039 (1967).  
<sup>2</sup>For a recent overview on this subject, see D. M. Newns, C. C. Tsuei, P. C. Pattnaik, and C. L. Kane, Comments Condens. Matter Phys. **15**, 273 (1992).  
<sup>3</sup>R. Combescot and J. Labbé, Phys. Rev. B **38**, 262 (1988).  
<sup>4</sup>G. D. Mahan, Phys. Rev. B **48**, 16 557 (1993).  
<sup>5</sup>J. E. Hirsch and D. J. Scalapino, Phys. Rev. Lett. **56**, 2732 (1986).  
<sup>6</sup>J. Labbé and J. Bok, Europhys. Lett. **3**, 1225 (1987).  
<sup>7</sup>C. C. Tsuei, D. M. Newns, C. C. Chi, and P. C. Pattnaik, Phys. Rev. Lett. **65**, 2724 (1990).  
<sup>8</sup>C. C. Tsuei, Physica A **168**, 238 (1990).  
<sup>9</sup>R. J. Radtke and M. R. Norman, Phys. Rev. B **50**, 9554 (1994).  
<sup>10</sup>A. B. Migdal, Sov. Phys. JETP **7**, 996 (1958).  
<sup>11</sup>G. M. Eliashberg, Sov. Phys. JETP **11**, 696 (1960).  
<sup>12</sup>H. R. Krishnamurthy, D. M. Newns, P. C. Pattnaik, C. C. Tsuei, and C. C. Chi, Phys. Rev. B **49**, 3520 (1994).  
<sup>13</sup>J. R. Schrieffer, J. Low Temp. Phys. **99**, 397 (1995).  
<sup>14</sup>L. Pietronero and S. Strässler, Europhys. Lett. **18**, 627 (1992).

- <sup>15</sup>C. Grimaldi, L. Pietronero, and S. Strässler, Phys. Rev. Lett. **75**, 1158 (1995).  
<sup>16</sup>L. Pietronero, S. Strässler, and C. Grimaldi, Phys. Rev. B **52**, 10 516 (1995).  
<sup>17</sup>C. Grimaldi, L. Pietronero, and S. Strässler, Phys. Rev. B **52**, 10 530 (1995).  
<sup>18</sup>A. A. Abrikosov, Physica C **244**, 243 (1995).  
<sup>19</sup>G. Grimvall, *The Electron-Phonon Interaction in Metals* (North-Holland, Amsterdam, 1981); D. J. Scalapino, in *Superconductivity*, edited by R. D. Parks (Dekker, New York, 1969), p. 449.  
<sup>20</sup>P. B. Allen and B. Mitrovic, in *Solid State Physics*, edited by H. Ehrenreich, F. Seitz, and D. Turnbull (Academic, New York, 1982), Vol. 37.  
<sup>21</sup>R. Combescot, Phys. Rev. B **42**, 7810 (1990).  
<sup>22</sup>V. N. Kostur and B. Mitrovic, Phys. Rev. B **50**, 12 774 (1994).  
<sup>23</sup>R. S. Markiewicz, Physica C **177**, 171 (1991).  
<sup>24</sup>P. A. Lee and N. Read, Phys. Rev. Lett. **58**, 2691 (1987).  
<sup>25</sup>J. Bok, Physica C **209**, 107 (1993).